Available online at www.sciencedirect.com

ScienceDirect

Ceramics International 39 (2013) 9665–9670

CERAMICS INTERNATIONAL

www.elsevier.com/locate/ceramint

Fabrication of zirconium oxide coatings on stainless steel by a combined laser/sol–gel technique

Y. Adraider[a,*], Y.X. Pang[a], F. Nabhani[a], S.N. Hodgson[a], M.C. Sharp[b], A. Al-Waidh[b]

[a]*School of Science and Engineering, Teesside University, Middlesbrough TS1 3BA, UK*
[b]*General Engineering Research Institute, Liverpool John Moores University, Byrom Street, Liverpool L3 3AF, UK*

Received 10 September 2012; received in revised form 21 May 2013; accepted 22 May 2013
Available online 30 May 2013

Abstract

A new route of combining sol–gel coating technology and laser processing is developed and used for manufacturing zirconia coatings on stainless steel substrates. In this method, sol–gel zirconia is first synthesised using zirconium (IV) *tert*-butoxide as precursor and a mixture of isopropanol and water as the solvent. The sol is coated on the substrate by dip-coating, and then the dried sol–gel coating is irradiated by a fibre laser at different energy densities ranging from 4.35 to 10.9 J/mm^2. Various techniques were applied to characterise the zirconia coatings on the substrate surfaces after laser treatment, including attenuated total reflectance Fourier transform infrared spectroscopy, X-ray diffraction, scanning electron microscopy, energy-dispersive spectroscopy and contact angle measurements. The results show that the fibre laser in continuous wave mode is effective to convert the as-dried amorphous xerogel coating on the substrate into zirconia coatings crystallised in tetragonal structure. The coating surface morphology varies with the laser energy densities and the highest coating uniformity is obtained at the lowest laser energy tested in this research.

Keywords: Sol–gel zirconia coatings; Fibre laser; Zirconium oxide; Stainless steel substrates

1. Introduction

The sol–gel method has been widely employed to prepare ceramic thin films, due to its low processing temperature and cost, excellent adhesion, high purity coatings and simplicity [1]. Sol–gel zirconia (ZrO_2) coatings are widely used as an excellent ceramic material to protect the metal surfaces against the corrosion and oxidation because of its unique thermal properties [2]. The thermal expansion coefficient of zirconia is close to most of the metals, which renders it to be a preferable substance for hard and protective coating applications such as metal cutting tools, corrosion resistance and nuclear energy reactors [3–5].

Zirconia can be found in three different crystal structures depending on the calcination temperatures, which are monoclinic (up to 1100 °C), tetragonal (1100–2370 °C) and cubic (above 2370 °C) [6]. It is reported that the stabilised tetragonal structure of zirconia is the preferable one for utilisation as a protective coating on stainless steel [7]. Various routes have been used to fabricate the zirconia coatings: sol–gel route [8], plasma sputtering [9], ultraviolet (UV) irradiation [10], and ultrasound assisted technique [11].

Recently, laser technology has become a popular tool in surface modification field due to its excellent advantages, namely the accurate control over laser parameters, the capability of generating a localised temperature rise on the surface and the treatment of substrate surface without affecting the bulk properties. Several researchers have reported depositing zirconium oxide thin films by means of laser technology. Al-Kuhaili and Durrani [12] reported the use of pulsed excimer laser to ablate ZrO_2 targets for depositing zirconium oxide thin films on silica substrates, and found that the deposited zirconium oxide thin films have an amorphous structure with large surface density. Flamini et al. [13] used similar technology to deposit ZrO_2 films on glass and quartz substrates by

*Corresponding author. Tel.: +44 7826702535.
E-mail address: F6098038@tees.ac.uk (Y. Adraider).

0272-8842/$ - see front matter © 2013 Elsevier Ltd and Techna Group S.r.l. All rights reserved.
http://dx.doi.org/10.1016/j.ceramint.2013.05.089

employing KrF and Nd:YAG laser to ablate ZrO_2 solid targets at different conditions, and the results demonstrate the validity of this technique to fabricate the ZrO_2 thin films for optical applications.

In this study, we reported the fabrication of zirconia coatings stabilised with 3 mol% Y_2O_3 (3YSZ) on stainless steel (AISI316) substrates by a combination of sol–gel technique and an ytterbium fibre laser (wavelength 1064 nm) processing technology. The resultant zirconia coatings on the substrate surfaces after laser irradiation are investigated using attenuated total reflectance Fourier transform infrared spectroscopy (ATR-FTIR), X-ray diffraction (XRD), scanning electron microscopy (SEM) and contact angle measurements. This method of depositing sol–gel zirconia coatings on the metal surfaces using laser irradiation is expected to be an effective technique for the engineering applications in the future.

2. Experimental

2.1. Sample preparation

The zirconia sols were synthesised as follows. Isopropanol (solvent, 45 g) and nitric acid (catalyst, 1.9 g) were charged in a flask and stirred for some time, and then zirconium (IV) *tert*-butoxide (precursor, 11.5 g) was dissolved in this mixture (isopropanol and nitric acid) under vigorous stirring at room temperature. After 2 h, distilled water (5.4 g) was slowly dropped into the solution and the system was constantly stirred for a few hours until the solution became transparent, indicating that a colloidal zirconia dispersion was formed. Yttrium acetate was dissolved in the mixture of isopropanol and nitric acid and then added to the zirconia sol to form a homogeneous solution containing 3 mol% yttrium acetate based on zirconium (IV) *tert*-butoxide. The sol was then ready for dip-coating. All chemicals were purchased from Sigma-Aldrich and used without further treatment.

The AISI316 sheet of 2 mm thickness was cut into 20 mm × 10 mm coupons and then polished with various grit SiC sand papers and finally 6 μm diamond paste. The polished substrates were cleaned by electrochemical degreasing, deionised water rinsing, and then dried in air at room temperature. The chemical composition of AISI316 is presented in Table 1.

The zirconia sol was coated on the AISI316 substrates through dip-coating technique at the same immersion and removal speed of 2.3 mm/s. The AISI316 substrates were dipped in the zirconia sol for duration of circa 60 s. The thickness of the zirconia coating applied on the substrates surfaces was circa 1.5 μm. All dip coated samples were dried in air at room temperature and then ready for laser treatment.

The laser treatment was performed with a fibre laser (SPI G3.0 Fibre Laser Module, SPI Lasers, UK) of a wavelength 1064 nm under the continuous wave mode (cw). The zirconia coated surfaces were irradiated over an area of 10 mm × 6 mm, via a GSI Lightning Galvanometer Scanning head and a 100 mm Linos f-theta focussing lens. The beam entering the scanning head was collimated to fill the scanning head aperture, leading to a nominal focussed spot diameter of 23 μm. The distance between the scanning lines was set at 20 μm to ensure that all the scanned area was irradiated with the laser. The laser energy densities used were 4.35 J/mm^2, 7.61 J/mm^2 and 10.9 J/mm^2.

2.2. Characterisation

The analysis of attenuated total reflectance Fourier transform infrared spectroscopy (ATR-FTIR) was performed on a Thermo Nicolet 5700 FTIR spectrometer. All spectra were conducted in a uniform range of wavenumbers between 400 and 4000 cm^{-1} at 4 cm^{-1} resolution, with averaging over 32 scans.

X-ray diffraction (XRD) was performed on a Siemens D500 X-ray diffractometer with CuKα radiation at 20 mA and 40 kV. The diffraction patterns were collected in the 2θ range from 20° to 70° with step size of 0.02° and step time 1 s.

Surface morphology and microstructure were observed with scanning electron microscopy (SEM, Hitachi 3400N, England). Elemental composition of zirconia coated surfaces was obtained using energy-dispersive spectroscopy (EDS) attached to the SEM.

Contact angle measurements were carried out by a drop shape analyser, DSA100 (KRUSS), using double distilled water as the determining medium.

3. Results and discussion

3.1. ATR-FTIR analysis

The ATR-FTIR analysis was applied to investigate the influence of the fibre laser irradiation on the chemical composition of the zirconia coatings on the AISI316 substrate. As shown in Fig. 1, the spectrum of as-dried coating (without laser treatment) has various absorption bands: the bands at 437 and 603 cm^{-1} correspond to Zr–O–Zr bonds [2]. The band located at 1521 cm^{-1} is related to Zr–O–C from the zirconium alkoxide, whilst the band centred at 1320 cm^{-1} is assigned to the NO_3 group originated from the nitric acid [14,15]. The absorption bands at 1618 cm^{-1} and 3300 cm^{-1} are attributed to the vibration of the hydroxyl groups and bonded water [16]. The bands in the range 1900–2400 cm^{-1} are due to the atmospheric absorption and are not significant. After laser

Table 1
Chemical composition of the AISI316 used.

C (%)	Mn (%)	Si (%)	P (%)	S (%)	Cr (%)	Mo (%)	Ni (%)	N (%)	Fe (%)
0.08	2.0	0.75	0.045	0.03	16.0–18.0	2.0–3.0	10.0–14.0	0.1	balance

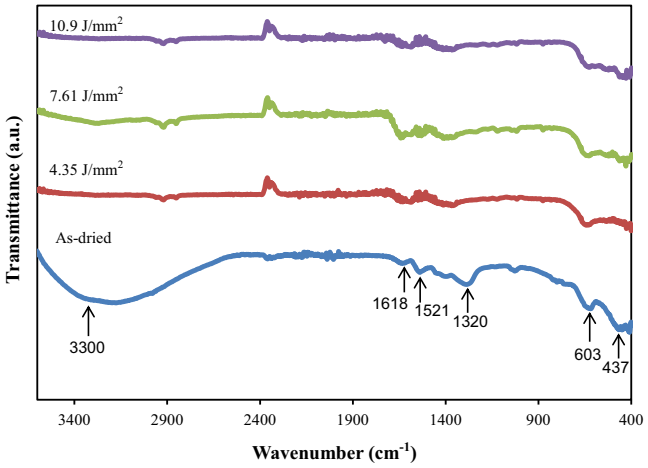

Fig. 1. ATR-FTIR spectra of zirconia coatings with and without laser irradiation.

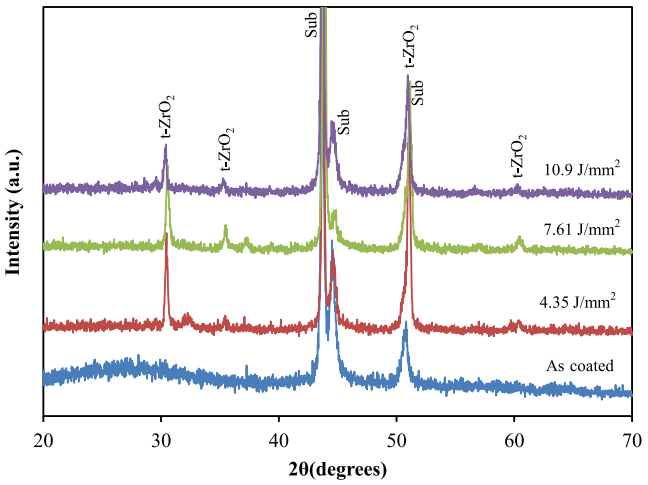

Fig. 2. XRD patterns of zirconia coatings processed at different laser energies.

irradiation, significant changes are observed. The bands at 1320 cm^{-1}, 1618 cm^{-1} and 3300 cm^{-1} have been completely eliminated, whilst the bands at 437 cm^{-1}, 603 cm^{-1} and 1521 cm^{-1} remain in all spectra after laser irradiation regardless of laser energy densities applied. The ATR-FTIR results indicate that laser irradiation causes a significant change on the chemical structure of the zirconia coatings.

3.2. X-ray analysis

X-ray diffraction patterns of the zirconia coatings on the substrates are depicted in Fig. 2. It can be seen that the XRD patterns for the laser irradiated zirconia coatings are quite different from those of the as-dried coating. There is a shallow hump spreading from 20° to 35° on the pattern of the as-dried coating, apart from the diffraction peaks at $2\theta = 43.6°$, 44.0° and 50.3° which belong to the stainless steel substrate [17], indicating that the coating is in an amorphous state. After laser exposure, a number of diffraction peaks characteristic of tetragonal phase of zirconia are detected, $2\theta = 30.2°$, 34.5°, 50.2° and 60.2°, irrespective of higher or lower laser energy density being applied [15,16]. However, the laser energy density has a certain influence on the intensity of the diffraction peaks, particularly for the peak at 30.2° which shows that the peak intensity varies inversely with the laser energy density. These XRD results are consistent with the ATR-FTIR results; both confirm that this fibre laser irradiation is effective in converting the as-dried (xerogel) amorphous coating into crystalline zirconia coatings.

3.3. Surface morphology

Surface morphology of the substrates coated with zirconia films was observed using scanning electron microscopy to study the influence of the fibre laser density. As shown in Fig. 3, surface morphology of the zirconia coatings is significantly different from those of the as-dried coating with visible laser tracks on the scanned coating surfaces as illustrated by the micrographs taken at low magnification. Apart from the tracks, there are some thick coating spots spread over the surface and their shape changes with the laser energy density applied. At the lowest laser energy density, the spots have an irregular shape, and change to more or less circular shape and then the strip elongated along with the laser track at laser energy densities of 7.61 J/mm^2 and 10.9 J/mm^2. Such a morphology is probably formed by laser induced melting and flow of the as-dried coating on the substrate. The coating is relatively uniform when processed at the lowest laser density of 4.35 J/mm^2, in comparison with those processed at higher laser energy densities, as can be seen from the images taken at higher magnification. This is because such a melting and flow effect becomes stronger with increasing laser energy density.

3.4. EDS analysis

The EDS analysis of the chemical composition of the zirconia coatings on the substrate surfaces after laser irradiation was performed at the spot and background areas which are indicated, respectively, as 1 and 2 in the micrographs of Fig. 3. The typical EDS spectra in areas 1 and 2 are depicted in Fig. 4 and the elemental composition for coatings processed at various laser energy densities is summarised in Table 2. It is observed that there is a significant difference of elemental composition between areas 1 and 2, with the zirconium content being much higher in area 1 than in area 2. This result suggests that the zirconia coating is present all over the substrate surface, though the amount is less in the background area. The higher zirconium content at area 2 for the sample processed at laser density 4.35 J/mm^2 (Table 2) indicates that this coating is more uniform than those processed at higher laser energy densities.

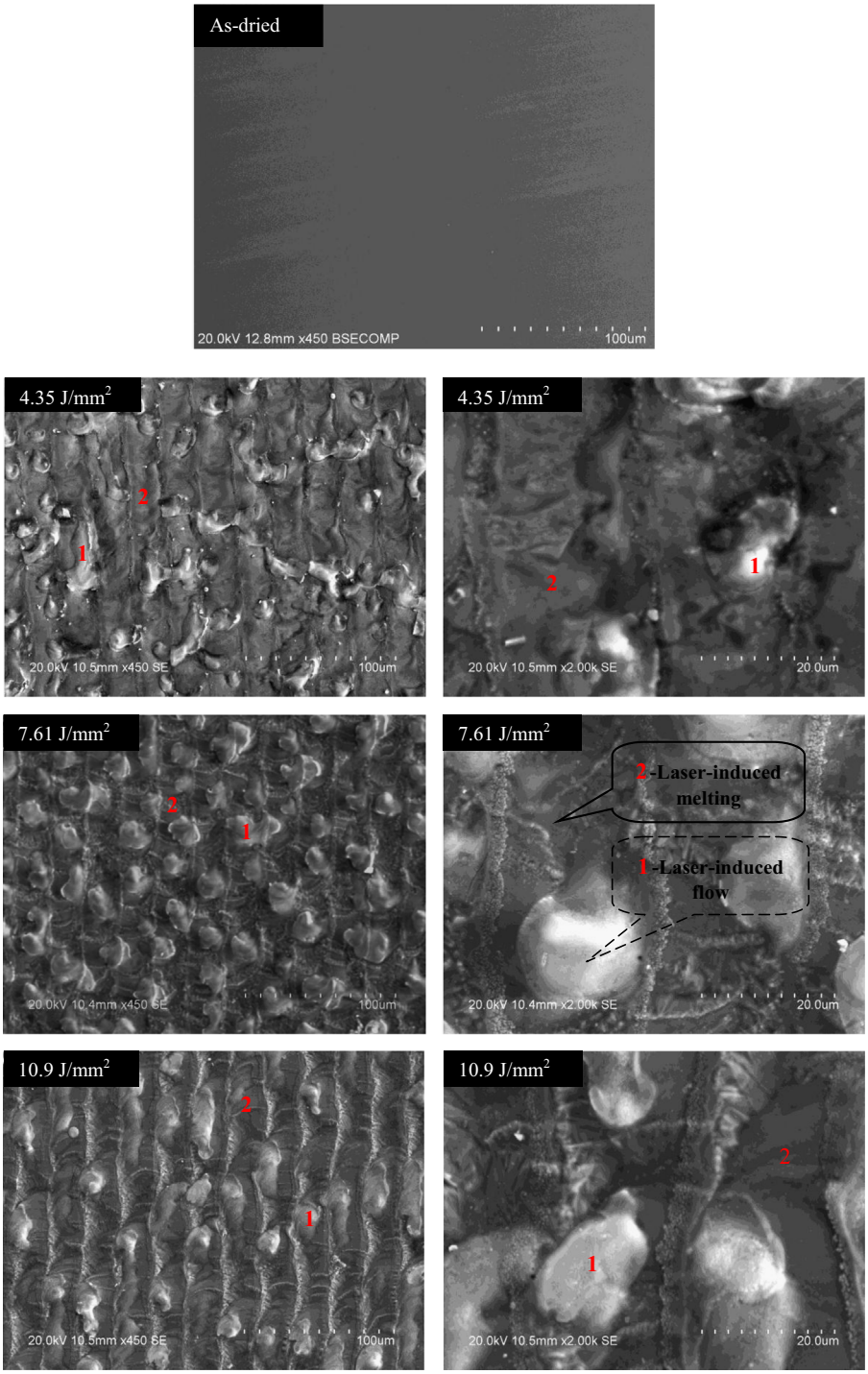

Fig. 3. SEM micrographs of zirconia coatings irradiated at various laser energies.

3.5. Surface properties

The surface property changes of zirconia coatings on the AISI316 surfaces were investigated by contact angle and interfacial tension (IFT) measurements. As shown in Fig. 5, these properties are significantly affected by laser treatment. The as-dried coating has contact angle and interfacial tension between the zirconia coating and water droplet circa $24.5 \pm 1^{\circ}$ and 125 ± 5 mN/m respectively, indicating that it has a highly hydrophilic surface. After laser exposure at energy density of 4.35 J/mm^2, the contact angle raises to $86.4 \pm 1^{\circ}$, whilst the interfacial tension decreases down to 43.8 ± 2 mN/m. With further increase of the laser energy densities to 7.61 J/mm^2 and 10.9 J/mm^2, no distinct variation is produced. Such a dramatic increase in contact angle comes from chemical composition change due to the conversion of xerogel coating into zirconia

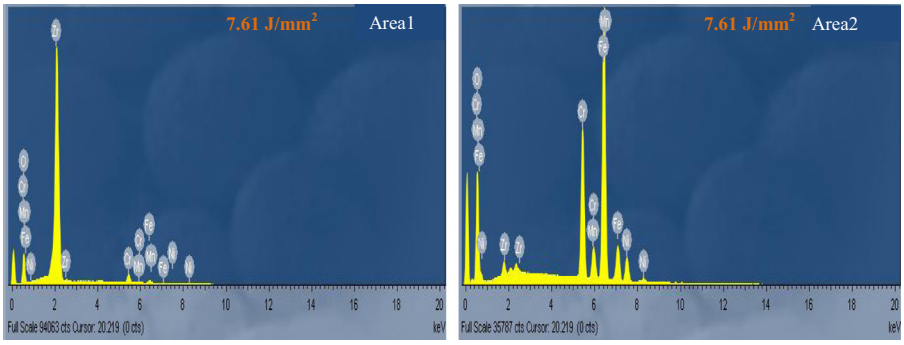

Fig. 4. EDS analysis of elemental composition: area 1 represents the laser induced flow and area 2 represents the laser induced melting.

Table 2
Elemental composition of zirconia coated surfaces.

Laser energy (J/mm^2)	Atomic%											
	Area 1						Area 2					
	O	Zr	Fe	Cr	Mn	Ni	O	Zr	Fe	Cr	Mn	Ni
4.35	63.07	27.06	1.02	8.85	–	–	25.96	8.42	42.37	14.65	1.90	6.70
7.61	62.12	25.30	1.04	11.22	0.18	0.14	36.19	1.42	40.59	14.28	1.95	5.57
10.9	65.58	12.14	3.49	14.03	4.76	–	61.75	1.43	15.88	14.02	4.95	1.97

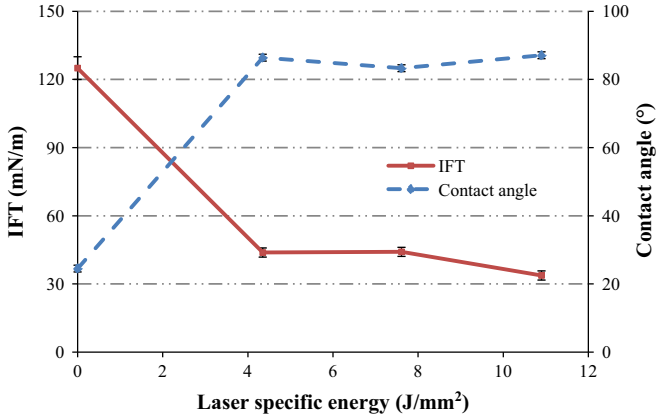

Fig. 5. Variation of water contact angle and IFT for zirconia coated surfaces with laser energies.

coating under laser exposure, and this is in agreement with the ATR-FTIR results (Fig. 1). In addition, the topography of the coating surfaces produced by the laser scanning also contributes to the increase of the contact angle after laser processing.

4. Conclusion

Zirconia coatings have been successfully produced on a stainless steel surface using a combined process of sol–gel technology and fibre laser irradiation under continuous wave mode. The ATR-FTIR analysis and contact angle measurements confirm that the laser treatments lead to the change of the as-dried sol–gel coating into zirconia coatings. The XRD results prove that the zirconia coatings crystallised in tetragonal structure are formed after laser irradiation at various energy densities. The SEM micrographs reveal that laser irradiation at different energy densities results in different surface morphologies due to two dominant effects: laser-induced flow and melting. The coating uniformity is better when processed at lower laser energy density and the coating covers the whole laser processed surface though the coating amount at area 1 is much higher than that in the background area.

References

[1] Y. Adraider., Y.X. Pang, F. Nabhani, S.N. Hodgson, Z.Y. Zhang, Laser-induced deposition of sol–gel alumina coating on stainless steel under wet condition, Surface and Coatings Technology 205 (2011) 5345–5349.
[2] F. Heshmatpour, R.B. Aghakhanpour, Synthesis and characterization of nanocrystalline zirconia powder by simple sol–gel method with glucose and fructose as organic additives, Powder Technology 205 (2011) 193–200.
[3] K. Koski, J. Holsa, P. Juliet, Properties of zirconium oxide thin films deposited by pulsed reactive magnetron sputtering, Surface and Coatings Technology 120–121 (1999) 303–312.
[4] M.J. Paterson, D.G. McCulloch, P.J.K. Paterson, B. Ben-Nissan, The morphology and structure of sol–gel derived zirconia films on stainless steel, Thin Solid Films 311 (1997) 196–206.
[5] H. Li, K. Liang, L. Mei, S. Gu, S. Wang, Oxidation protection of mild steel by zirconia sol–gel coatings, Materials Letters 51 (2001) 320–324.
[6] R. Dwivedi, A. Maurya, A. Verma, R. Prasad, K.S. Bartwal, Microwave assisted sol–gel synthesis of tetragonal zirconia nanoparticles, Journal of Alloys and Compounds 509 (2011) 6848–6851.

[7] N. Garg, V.K. Mittal, S. Bera, A. Dasgupta, V. Sankaralingam, Preparation and characterization of tetragonal dominant nanocrystalline ZrO_2 obtained via direct precipitation, Ceramics International 38 (2012) 2507–2512.
[8] L. Liang, Y. Xu, D. Wu, Y. Sun, A simple sol–gel route to ZrO_2 films with high optical performances, Materials Chemistry and Physics 114 (2009) 252–256.
[9] Y. Ohtsu, M. Egami, H. Fujita, K. Yukimura, Preparation of zirconium oxide thin film using inductively coupled oxygen plasma sputtering, Surface and Coatings Technology 196 (2005) 81–84.
[10] J.J. Yu, J.Y. Zhang, I.W. Boyd, Formation of stable zirconium oxide on silicon by photo-assisted sol–gel processing, Applied Surface Science 168 (2002) 190–194.
[11] K. Prasad, D.V. Pinjari, A.B. Pandit, S.T. Mhaske, Synthesis of zirconium dioxide by ultrasound assisted precipitation: effect of calcination temperature, Ultrasonics Sonochemistry 18 (2011) 1128–1137.
[12] M.F. Al-Kuhaili, S.M.A. Durrani, Effect of annealing on pulsed laser deposited zirconium oxide thin films, Journal of Alloys and Compounds 509 (2011) 9536–9541.
[13] C. Flamini, A.G. Guidoni, R. Teghil, V. Marotta, Zirconium oxide films deposited by reactive pulsed laser ablation, Applied Surface Science 138–139 (1999) 344–349.
[14] E. Nouri, M. Shahmiri, H.R. Rezaie, F. Talayian, A comparative study of heat treatment temperature influence on the thickness of zirconia sol–gel thin films by three different techniques: SWE, SEM and AFM, Surface Coatings Technology 206 (2012) 3809–3815.
[15] S.K. Tiwari, J. Adhikary, T.B. Singh, R. Singh, Preparation and characterization of sol–gel derived yttria doped zirconia coatings on AISI 316L, Thin Solid Films 517 (2009) 4502–4508.
[16] V.G. Deshmane, Y.G. Adewuyi, Synthesis of thermally stable, high surface area, nanocrystalline mesoporous tetragonal zirconium dioxide (ZrO_2): effects of different process parameters, Microporous and Mesoporous Materials 148 (2012) 88–100.
[17] C. Pflitsch, D. Viefhaus, U. Bergmann, B. Atakan, Organometallic vapour deposition of crystalline aluminium oxide films on stainless steel substrates, Thin Solid Films 515 (2007) 3653–3660.